Proceedings of the 8th World Congress on Momentum, Heat and Mass Transfer (MHMT'23)
Lisbon, Portugal – March 26 – 28, 2023
Paper No. ICMFHT 135
DOI: 10.11159/icmfht23.135

Flow Boiling Instabilities and Single-Phase Pressure Drop in Rectangular Microchannels with Different Inlet Restrictions

Mark Schepperle[1], Aum Mandal[1], Peter Woias[2]
[1]Laboratory for Design of Microsystems, Department of Microsystems Engineering, University of Freiburg
Georges-Koehler-Allee 102, 79110 Freiburg, Germany
schepperle@imtek.de; woias@imtek.de

Abstract – Flow instabilities are one of the main challenges in the field of microchannel flow boiling. They modify the hydrodynamics and can lead to premature critical heat flux (CHF). To overcome these instabilities, geometrical adjustments such as inlet constrictions have proven to be very effective. Notwithstanding the effectiveness of these structures in preventing instabilities, so far only a few inlet restrictions have been discussed in the literature. For this reason, two different restrictions to suppress flow boiling instabilities were tested in this work and compared to a channel configuration without restriction. In addition, the single-phase pressure drop was measured to determine the impact of the restrictions on the pressure loss at the inlet. In all experiments, degassed DI water was used as working fluid and the mass flow rate ranged from 0.95 to 67.62 g/min. The heating power was 0 W for the adiabatic single-phase pressure measurements and 12 W for the flow-boiling instability studies. It was found that only one of the two inlet modifications could prevent flow boiling instabilities such as bubble clogging and flow reversal. At the same time, the part of this restriction that was crucial for flow stabilization had the least effect on the single-phase pressure drop in the microchannel.

***Keywords*:** Microchannel; Two-phase; Flow boiling; Instabilities; Inlet restriction; Single-phase; Pressure drop; DI water

1. Introduction

The ongoing miniaturization of high-performing electronic devices leads to a significant increase in heat flux density (e.g. up to 12-45 MW/m^2 for local hot spots in computer chips). This heat must somehow be effectively dissipated [1]. One of the most promising solutions for dissipating this high heat flux is to utilize the latent heat of two-phase flow boiling in microchannels [2]. Microchannel flow boiling is characterized not only by its highly effective cooling capability, but also by uniform chip temperature distribution and high hot-spot cooling performance [3].

In spite of the many advantages of microchannel flow boiling, they are still not used in commercial applications. The primary reason for this is that there are still many fundamental issues that have not been solved [1]. These include, above all, the suppression of flow instabilities. These unstable behaviours can lead to a significant reduction in heat transfer and to dry-out as well as boiling crises [2]. In recent years, flow instabilities in microchannels have been intensively studied [4]. It has been found repeatedly that geometric modifications such as inlet restrictions are among the most effective methods of flow instability suppression [5]. However, only a few types of inlet restrictions have been tested so far. Moreover, these were almost exclusively horizontally constraining. There are also few studies that compare different inlet modifications, as it is the case e.g. in [6].

For this reason, the objective of this paper was to investigate two inlet restrictions and to evaluate their effectiveness in suppressing instabilities during two-phase flow boiling in microchannels. As a novelty compared to previously published studies, the channel cross-section was constricted in vertical direction in one of the two restrictions. The comparison of the two tested modifications was intended to provide new clues about the optimal design of such structures and to answer whether vertical constrictions at the channel inlet are as suitable as constrictions in horizontal direction.

2. Description of the Experiment

This section explains the experimental setup with the different microchannel versions that was used for the flow instability analysis and the single-phase pressure drop measurements. This is followed by a brief description of the employed methods and the calculation of the pressure losses across the inlet constrictions.

2.1. Experimental Setup

The experimental apparatus used for the experiments was already utilized in similar configurations in [7-9] and consisted of the following components: Reservoir to provide DI water; micro annular gear pump to supply DI water to the microchannel; 10 µm particle filter in front of the micropump to prevent contaminants from entering the test section; degasser to degas the DI water; reactor with integrated microchannel (Figure 1 (a)), cartridge heaters inserted in holes at the microchannel bottom (Figure 1 (b)) to heat up the microchannel and initiate flow boiling; differential pressure transducer with compensated line pressure and compensated temperature dependency to measure the pressure drop across the microchannel; wastewater reservoir; high-speed camera mounted above the observation window to investigate flow boiling instabilities in the microchannel. Figure 1 illustrates the reactor assembly, in which the aforementioned observation window can be seen, in an exploded view (a), the microchannel without constriction in a top/bottom view and the two different inlet restrictions of the other two microchannels in a slightly tilted cross-sectional view (c)-(d). The spring probes and Pt microheaters shown in Figure 1 (a) have been part of the setup however they were not relevant for the experiments performed in this work.

All microchannels tested were 65 mm long, 1.5 mm wide and 0.5 mm high with a hydraulic diameter of 0.75 mm. They were manufactured in stainless steel (1.4404/316L) by machining. The inlet and outlet holes of the microchannel without restriction (Figure 1 (b)) had a diameter of 1.5 mm. The inlet holes of the two channels with restrictions had a diameter of 0.5 mm (Figure 1 (c)-(d)) the outlet holes had a diameter of 1.5 mm as for the channel without restriction. This reduced inlet diameter of 0.5 mm already represented the first tested restriction R1 (Figure 1 (c)). In the second restriction R2 (Figure 1 (d)), the channel height in the immediate vicinity of the inlet hole was additionally reduced vertically by half to 0.25 mm.

For each experiment, one of these microchannels was inserted into the cavity in the middle of the reactor housing (Figure 1 (a)). An O-ring in a trench around the microchannel provided a watertight seal between the microchannel and the glass lid. DI water was supplied and discharged through the two holes at the ends of the milled microchannels, each leading to an inlet and outlet on the reactor housing. The inlet and outlet of the reactor met through holes inside the reactor that led the DI water to the pressure transducer ports and the inlet/outlet of the microchannel.

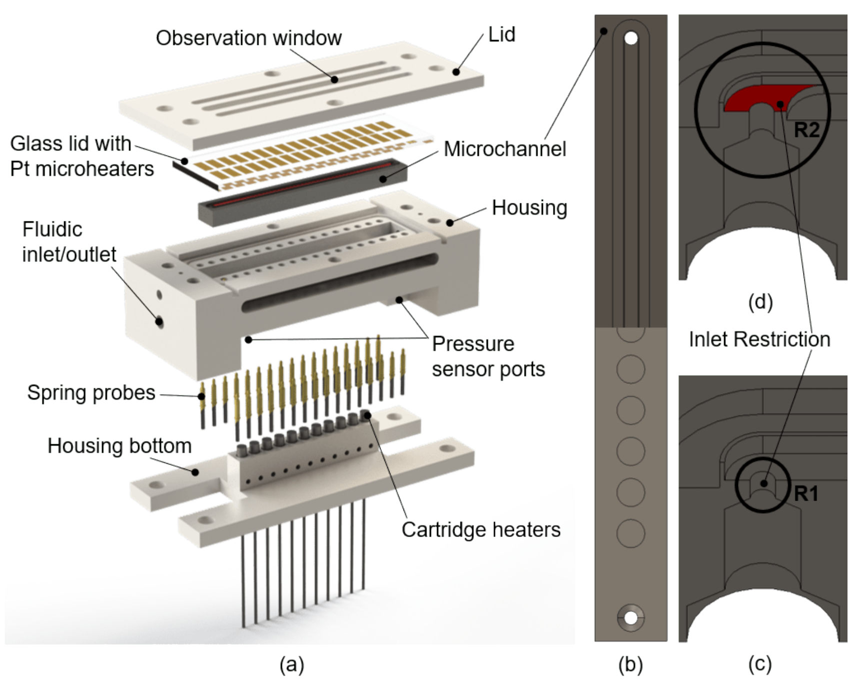

Fig. 1: (a) 3D CAD drawing of the reactor system for flow boiling instability analysis and single-phase pressure drop measurements; (b) top/bottom view of the microchannel without constriction; (c)-(d) cross-sectional view of the tested inlet restrictions R1 and R2.

2.2. Microchannel Flow Boiling Instability Analysis

Flow instabilities such as bubble clogging and flow reversal were determined optically via videos recorded at 2000 fps fps with a high-speed camera. A low mass flow rate of 1.5 g/min was chosen. Furthermore, degassed DI water was introduced introduced into the channel at a subcooled temperature of 22.5 ± 0.5 °C. The water heated up to boiling temperature through through the heating cartridges until the second half of the microchannel, where vapor bubble formation and flow boiling instabilities finally occurred. The second half of the channel was also where the videos for the instability analysis were recorded. In all experiments, the total heating power of the cartridge heaters was 12 W. For thermal insulation, the entire reactor was wrapped with glass wool. Only in the observation window area (Figure 1 (a)) was a glass wool free area present to allow the flow boiling process to be observed.

2.3. Single-Phase Pressure Drop and Inlet Pressure Loss

The single-phase pressure drop was determined under adiabatic conditions (23 ± 0.5 °C room temperature) for mass flow rates from 0.95 to 67.62 g/min for all microchannel configurations. The cartridge heaters at the microchannel bottom were not heated. The differential pressure measured via the pressure sensor ports ($\Delta p_{measured}$) includes the pressure loss at the channel inlet (Δp_{inlet}) and the pressure recovery at the channel outlet. The pressure recovery at the outlet was negligible, so it did not need to be considered. To obtain the pressure drop across the microchannel, the measured values must still be corrected as shown in the following equation:

$$\Delta \mathrm{p}_{\mathrm{mc}} = \Delta \mathrm{p}_{\mathrm{measured}} - \Delta \mathrm{p}_{inlet} \tag{1}$$

The inlet pressure losses were calculated with the data reduction method of Lee and Garimella (2008) [10]:

3. Results and Discussion

Figure 2 shows meaningful frames of the flow boiling process in the microchannel with restriction R1 (a)-(b) and the microchannel with restriction R2 (c) at 12 W total heating power and a mass flow rate of 1.5 g/min. Figure 2 (a)-(b) clearly shows flow instabilities such as flow reversal (a) and bubble clogging (b). Thus, restriction R1 is not suitable for the suppression of instabilities. The flow pattern is similar to that of the channel without restriction, which is why Figure 2 (a)-(b) can be considered representative of both channels (without restriction and with restriction R1). No flow instabilities were observed in the microchannel with restriction R2. The flow pattern resembled a stable slug/annular flow as it can be clearly seen in Figure 2 (c). Under the given process conditions, restriction R2 was therefore suitable for stabilizing boiling flow.

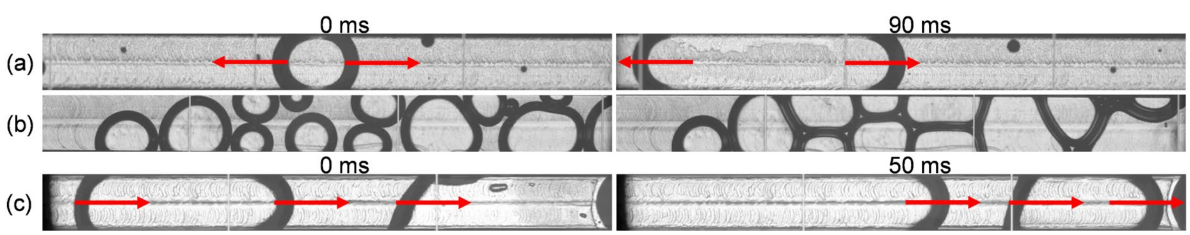

Fig. 2: Microchannel flow boiling at 12 W total heating power and a mass flow rate of 1.5 g/min: (a) flow reversal and (b) bubble clogging in the microchannel with restriction R1; (c) stable slug/annular flow in the microchannel with restriction R2.

The single-phase pressure drop of all microchannel configurations is shown in Figure 3, once the pure measured data ($\Delta p_{measured}$) in (a) and once the data corrected with the data reduction from [10] as Δp_{mc} (calculated with Equation 1) in (b). As can be clearly observed in Figure 3 (a), the restrictions R1 and R2 significantly increase the measured pressure drop. However, there is not much difference between the measured pressure drop R1 and R2. This suggests that the additional channel height reduction in vertical direction in the immediate vicinity of the inlet hole does not have a large effect on the measured pressure drop. Since restriction R1 did not show any improvement with respect to the instabilities, it can be assumed that restriction R2 leads to flow stabilization even without the inlet hole constriction from 1.5 to 0.5 mm and only with the vertical cross-sectional constriction in the flow region of the channel. For this reason, another theoretical restriction R3 has been added to Figure 3, which is intended to illustrate the probable behaviour of the pressure drop of restriction R2 without the narrowing of the inlet hole. The pressure drop of R3 was calculated by adding the difference of the measured data of R2 and R1 with the measured data of the channel without constriction. Figure 3 (b) confirms that the increased pressure drop in the channels with R1 and R2 is caused by the restrictions, since the pressure recovery at the outlet was negligible and after data reduction all pressure drop curves were similar.

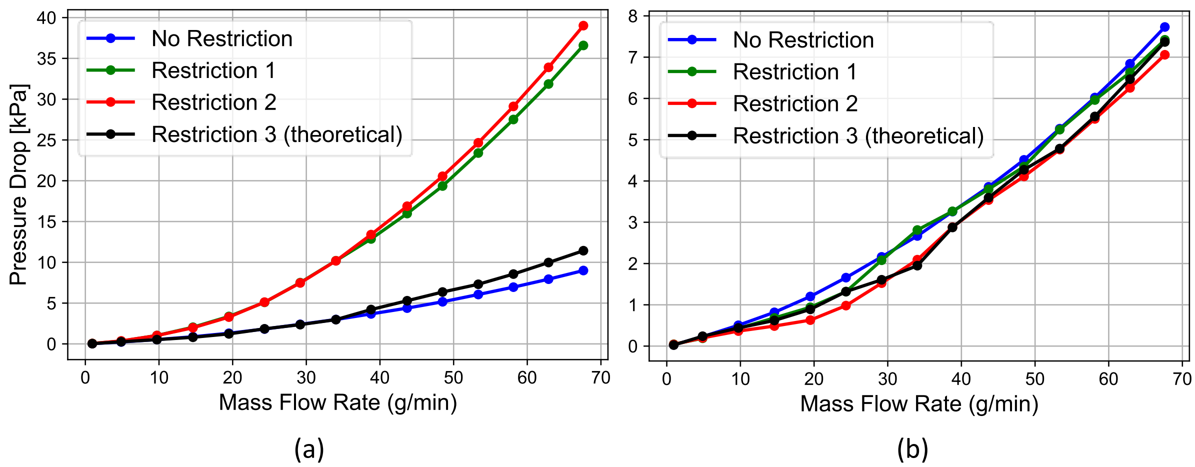

Fig. 3: Single-phase pressure drop of the microchannels with different restrictions: (a) as raw measurement data without considering inlet pressure losses; (b) as corrected measurement data with considering inlet pressure losses.

4. Conclusion

In summary, it can be said that vertical inlet restrictions in the flow cross-section of the microchannel are just as suitable for stabilizing boiling flows as horizontal ones. Furthermore, the increase in pressure drop caused by pressure losses across such a restriction is negligibly small and thus similar to the results of other publications such as [11], where they used horizontal restrictions in the immediate vicinity of an inlet plenum to suppress flow boiling instabilities in a micro-pin fin evaporator. Restricting the inlet hole, which is not in the direct flow cross-section of the microchannel, had no effect on flow boiling instabilities. At the same time, however, such a restriction generates large pressure losses, which leads to an extraordinary increase in the measured pressure drop. From this it can be further concluded that the flow-stabilizing effect of inlet restrictions is not brought about by increasing the fluidic resistance. Otherwise, the stabilization would be directly related to the increase in pressure drop across such a restriction.

Acknowledgements

Funding: This work was supported by the German Research Foundation (DFG) through the Research Unit 2383 ProMiSe under Grant No. WO 883/24-2.

References

[1] T. G. Karayiannis and M. M. Mahmoud, "Flow boiling in microchannels: Fundamentals and applications," *Appl. Thermal Eng.*, vol. 115, pp. 1372-1397, 2017.

[2] L. Cheng and G. Xia, "Fundamental issues, mechanisms and models of flow boiling heat transfer in microscale channels," *Int. J. Heat Mass Transf.*, vol. 108, part A, pp. 97-127, 2017.

[3] B. Agostini, M. Fabbri, J. E. Park, L. Wojtan, J. R. Thome and B. Michel, "State of the art of high heat flux cooling technologies," *Heat Transf. Eng.*, vol. 28, issue 4, pp. 258-281, 2007.

[4] G. Wang, P. Cheng and H. Wu, "Unstable and stable flow boiling in parallel microchannels and in a single microchannel," *Int. J. Heat Mass Transf.*, vol. 50, issues 21-22, pp. 4297-4310, 2007.

[5] Y. K. Prajapati and P. Bhandari, "Flow boiling instabilities in microchannels and their promising solutions–A review," *Exp. Therm. Fluid Sci.*, vol. 88, pp. 576-593, 2017.
[6] G. Wang, P. Cheng and A. E. Bergles, "Effects of inlet/outlet configurations on flow boiling instability in parallel microchannels," *Int. J. Heat Mass Transf.*, vol. 51, issue 9-10, pp. 2267-2281, 2008.
[7] M. Schepperle, M. Ghanam, A. Bucherer, T. Gerach and P. Woias, "Noninvasive platinum thin-film microheater/temperature sensor array for predicting and controlling flow boiling in microchannels," *Sens. Actuator A Phys.*, vol. 345, p. 113811, 2022.
[8] M. Schepperle, N. Samkhaniani, M. Magnini, P. Woias and A. Stroh, "Thermohydraulic Characterization of DI Water Flow in Rectangular Microchannels By Means Of Experiments and Simulations," in *Proceedings of the 7th World Congress on Momentum, Heat and Mass Transfer (MHMT'22)*, Virtual, 2022.
[9] M. Schepperle, S. Junaid, A. Mandal, D. Selvam and P. Woias, "Determination of Void Fraction in Microchannel Flow Boiling Using Computer Vision," in *Proceedings of the 8th World Congress on Mechanical, Chemical, and Material Engineering (MCM'22)*, Prague, Czech Republic, 2022.
[10] P.-S. Lee, S. V. Garimella, "Saturated flow boiling heat transfer and pressure drop in silicon microchannel array," *Int. J. Heat Mass Transf.*, vol. 51, issue 3-4, pp. 789-806, 2008.
[11] C. Falsetti, H. Jafarpoorchekab, M. Magnini, N. Borhani and J. R. Thome, "Two-phase operational maps, pressure drop, and heat transfer for flow boiling of R236fa in a micro-pin fin evaporator," *Int. J. Heat Mass Transf.*, vol. 107, pp. 805-819, 2017.